Jour of the KGS Vol. 16, No 3, June 2000, pp 5~13

Disturbed State Modeling for Dynamic Analysis of Soil-Structure Interface

흙-구조물 경계면의 동역학적해석을 위한 교란상태 모델링

Park, Inn-Joon[*1] 박 인 준
Yoo, Ji-Hyeung[*2] 유 지 형
Kim, Soo-Il[*3] 김 수 일

요 지

본 연구에서 흙(사질토)-구조물의 경계면에 대한 거동특성을 분석하기 위하여 교란상태개념(DSC)을 수정 및 보완하였다. 제안한DSC모델에서는 변형중인 재료는 상대적으로 손상되지 않은 상태(RI)와 완전 파괴된 상태(FA)가 혼합되어 있다는 가정에 기초를 두고있다. RI 상태는 HiSS모델을 이용하였고, FA상태는 한계상태모델을 이용하였다. 이런 DSC 모델을 Biot이론에 기초한 기존 유한요소 프로그램에 접목하였다. 본 연구에서 수정한 유한요소 프로그램을 이용하여 실제 경계면 실험(두 가지 하중조건: 정하중, 동하중)에 대하여 모의실험을 수행하였다. 또한 그 결과와 실내시험결과를 비교 검토하였다. DSC모델을 이용한 유한요소해석은 실제 실내시험 결과와 유사한 경향을 보였다. 본 연구의 결과를 통하여, DSC모델은 흙-구조물 경계면 해석에 비교적 합리적인 결과를 제공한다고 판단된다.

Abstract

In this study, the Disturbed State Concept (DSC) constitutive model is calibrated and modified for steel-sand interface by using the HiSS model for relative intact (RI) state and the critical state model for the fully adjusted (FA) part in the material. The general formulation for implementation is developed. Then, the DSC model with modification for interface is implemented in finite element program based on the generalized Biot's theory. The interface test under one-way monotonic and two-way cyclic loading were numerically simulated using the finite element program modified in this study. The DSC predictions show improved agreement with the observed results from laboratory test. Overall, the computer procedure with the DSC allows relatively improved simulation of the soil-structure interaction problems.

Keywords : Disturbed state concept, Soil-structure interaction, Relative intact state, Fully adjusted state, Finite element program

1. Introduction

Major problems associated predicting soil-structure interaction behavior are based on the fact that soil is neither homogeneous nor elastic and soil properties are spatially variable. There also exist significant coupling problems between the behavior of the structure and geologic media. When designing foundation or other geotechnical structures, the load transfer between the soil and structure takes place at the contact surface. This surface is called the *interface*. The behaviors of interface play an important role in the load-deformation response of soil-structure interaction systems.

The purpose of this study is to develop improved model

*1 Member, Post-Doctor, Dept. of Civil Engrg. Yonsei Univ
*2 Member, Associate Professor, Dept. of Civil Engrg. Kyungil Univ
*3 Member, Professor, Dept. of civil Engrg. Yonsei, Univ.

for simulation of saturated sand-structure interface behavior based on a general concept, called the *disturbed state concept* (DSC), which can characterize the behavior of saturated soils. The initial idea for this theory was introduced by Desai (1974) to characterize the softening response of an over-consolidated soil by expressing

the observed response in terms of its response in its normally consolidated state as the reference state. DSC model has been successfully verified with respect to other materials such as dry sands (Armaleh and Desai, 1990) and liquefaction of saturated sand (Desai et al., 1998; Park, 1997). In this study, DSC model is calibrated with respect to laboratory tests such as cyclic multi-degree-of-freedom shear test (CYMDOF) for the saturated interface. The model can be implemented in a dynamic nonlinear finite element procedure for coupled soil-fluid response toward solution of a typical boundary value problem such as simulation of test behavior of steel-sand interface.

2. Disturbed State Concept (DSC) Model

Details of the disturbed state concept (DSC) are introduced in various references (Armaleh and Desai, 1990; Desai et al., 1997; Park, 1997; Desai et al., 1998). In this paper, a brief description is presented with focusing on incremental formulations for implementation of finite element analysis.

The DSC is based on the idea that any stage during deformation of a material element is composed of a mixture of materials in two stages; relative intact (RI) stage and fully adjusted (FA) stage. The disturbances due to external load can involve particle motions and self-adjustment of the microstructure leading to micro-cracking and softening, and stiffening. As a consequence, the material in the RI state is transforming into the FA state at randomly disturbed locations (see Fig. 1). The coalescence of the FA clusters can lead to critical extent or to shear bands, causing instability (liquefaction) and failure.

The RI response can be characterized by using continuum theories such as elasticity and elasto-plasticity. The FA state can be defined as critical state concept that

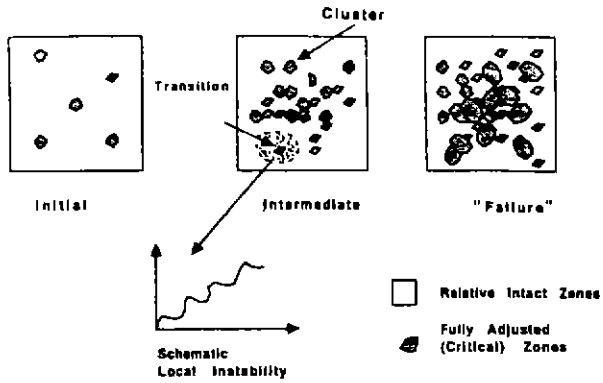

Fig 1 Schematic of orowth of the fully adjusted state (Park, 1997)

can carry shear reached up to that state for given initial hydrostatic pressure and deform in shear under constant volume, like a constrained liquid-solid (Roscoe, et al., 1958).

2.1 Idealization of an Interface

An interface is a thin layer between two contacting materials, through which the two materials intact. This layer poses different material properties than those of the neighboring interval. The interface is assumed to be a planar surface with an average thickness, t. By defining an appropriate interface thickness, the displacements can be converted into strain. The normal strain (ε_n) and the tangential strain (γ) can be written, respectively, as (see Fig. 2)

$$\varepsilon_n = \frac{v_r}{t} \tag{1}$$

$$\gamma = \frac{u_r}{t} \tag{2}$$

where v_r is the normal displacement and u_r is the relative shear displacement. Interface stresses are the

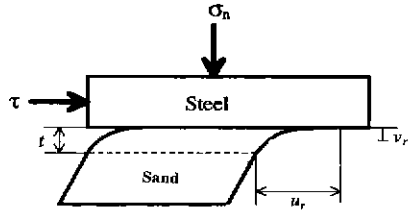

Fig. 2 Interface definition

average applied forces over the nominal planar area of the interface. The stresses at the interface are the tangential stress, τ, and the normal stress, σ_n. If T and N are the tangential and normal forces, respectively, and A_0 is the nominal interface area, the shear stress, τ, and the normal stress, σ_n, can be written as

$$\tau = \frac{T}{A_0} \tag{3}$$

$$\sigma_n = \frac{N}{A_0} \tag{4}$$

The interfaces in this study were subjected to constant normal and one-way monotonic/two-way cyclic shear stresses.

2.2 Relative Intact State

The relative intact state is described using an elasto-plastic model. In the context of plasticity, the yield function in written as

$$F = \left(\frac{\tau}{P_a}\right)^2 + \alpha\left(\frac{\sigma_n}{P_a}\right)^n - \bar{\gamma}\left(\frac{\sigma_n}{P_a}\right)^2 = 0 \tag{5}$$

where τ is the shear stress, σ_n is the effective normal stress, p_a is the atmospheric pressure, $\bar{\gamma}$ and n are model parameters, and α is the hardening function. The hardening function, α, can be defined in terms of the deviatoric plastic strain trajectory, ξ_D, and can be written as:

$$\alpha = \frac{h_1}{\xi_D^{h_2}} \tag{6}$$

where h_1 and h_2 are model parameters. For smooth interfaces the dominant plastic strains, ξ_D can be defined as

$$\xi_D = \int \sqrt{d\gamma^p d\gamma^p} \tag{7}$$

The line connecting the peaks of the yield surface is called the phase change line. At these points of maximum value, $\frac{\partial F}{\partial \sigma_n}$ is equal to zero. By applying to *Eq.* (5) and with appropriate manipulations, we can obtain:

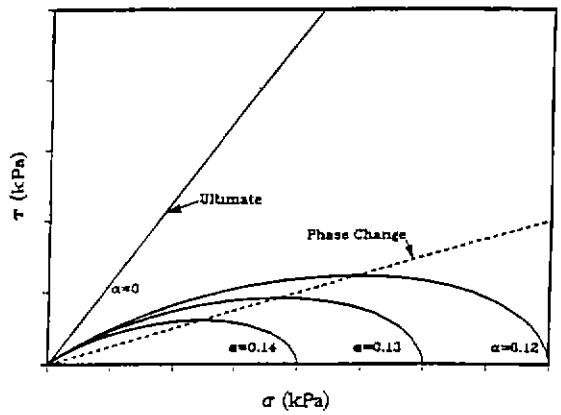

Fig. 3 Yield surface in $\tau - \sigma_n$ plane

$$\frac{\tau}{\sigma_n} = \sqrt{\bar{\gamma}\frac{(n-2)}{n}} \tag{8}$$

By looking at Fig. 3, the phase change line has a slope of $\sqrt{\bar{\gamma}\frac{(n-2)}{n}}$.

The ultimate surface in the τ vs. σ_n plot represents asymptotic states of given failure can be found from equation by setting α to zero:

$$\tau_{ult} = \sqrt{\bar{\gamma}}\,\sigma_n \tag{9}$$

The slope of the ultimate surface is $\sqrt{\bar{\gamma}}$ and it passes through zero, as seen in Fig. 3. The intact incremental stress-strain relationships were derived from the traditional elasto- plasticity formulation procedure. The constitutive relationship can be written as

$$\{d\sigma^i\} = [C^{ep}]\{d\varepsilon^i\} \tag{10}$$

2.3 Fully Adjusted State

This state is modeled following the critical state concepts in soil where shear displacements can continue without any changes in volume. The critical shear stress is proportional to the normal stress and can be written as

$$\tau^c = \bar{m}\sigma_n^c \tag{11}$$

where $\overline{m}$ is the slope in τ vs. σ_n fields, and the superscript c refers to the critical state condition. And the critical void ratio e^c may be defined as

$$e^c = e_\lambda - \lambda \ln \frac{\sigma_n^c}{P_a} \tag{12}$$

In the plot of e vs. $\ln \frac{\sigma_n}{P_a}$, e_λ is the void ratio at the atmospheric pressure, P_a, and λ is the slope in e vs. σ_n plot.

2.4 Disturbance Function

The disturbance function can be defined as

$$D = \frac{M_s^c}{M_s} \tag{13}$$

where M_s^c is the mass of solids in the FA state and M_s is the total mass of solids in the materials. Initially with no disturbance the material is assumed to be entirely in the RI state, therefore D equals to zero. With full disturbance the material can be assumed to be fully in the FA state, and at the ultimate state, $D = D_u \leq 1$.

The disturbance function, D, used in the current study is given by Armaleh and Desai (1990):

$$D = D_u \left[1 - e^{\left(-A\xi_D^Z\right)}\right] \tag{14}$$

where A, Z, and D_u are material parameters. Where D_u is often assumed to be unity. Fig. 4 shows a schematic of the disturbance function.

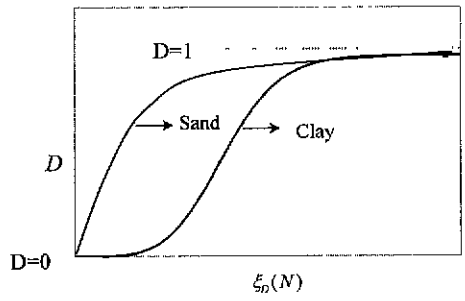

Fig. 4 Schematic of DSC function

2.5 Incremental Formulation for the DSC

Based on the equilibrium forces in the observed, RI, and FA states, the incremental constitutive equations to describe the observed response are derived as (Park, 1997; Desai *et al*, 1998)

$$d\sigma_{ij}^a = (1-D)d\sigma_{ij}^i + Dd\sigma_{ij}^c + dD(\sigma_{ij}^c - \sigma_{ij}^i) \tag{15}$$

where superscripts **a**, **i**, and **c** denote observed, relative intact, and critical state, respectively. Substituting Eq. (10), Eq. (11), and Eq. (12) into Eq. (15) for deriving the general incremental relationship between stress and strain, and let the following increments of the stress and strain be defined as $\begin{Bmatrix} d\sigma_n \\ d\tau \end{Bmatrix} = d\sigma_{ij}$ and $\begin{Bmatrix} d\varepsilon_n \\ d\gamma \end{Bmatrix} = d\varepsilon_{ij}$. Finally, the general incremental relations are derived as

$$d\sigma_{ij}^a = \Omega_{ijkl} d\varepsilon_{kl}^i + \Psi_{ijkl} d\varepsilon_{kl}^c + dD(\sigma_{ij}^c - \sigma_{ij}^i) \tag{16}$$

If it is assumed that all the strains in each reference state are equal ($d\varepsilon_{ij}^a = d\varepsilon_{ij}^i = d\varepsilon_{ij}^c$), Eq. (16) gives the DSC incremental stress-strain equations,

$$d\sigma_{ij}^a = (\Omega_{ijkl} + \Psi_{ijkl}) d\varepsilon_{kl}^i + dD(\sigma_{ij}^c - \sigma_{ij}^i) \tag{17}$$

where

$$\Omega_{ijkl} = (1-D)C_{ijkl}^{ep} + D\frac{\overline{m}}{\sqrt{J_{2D}^i}} J_1^c \left[\left(C_{ijkl}^{ep} - \frac{1}{3}\delta_{ij} C_{mmkl}^{ep}\right) - \left(\frac{S_{ij}^i S_{ij}^i}{2J_{2D}^i} C_{ijkl}^{ep}\right)\right] \tag{18}$$

$$\Psi_{ijkl} = D\frac{(1+e_0)}{\lambda} J_1^c \left[\frac{\overline{m} S_{ij}^i}{\sqrt{J_{2D}^i}} + \frac{1}{3}\delta_{ij}\right]\delta_{kl} \tag{19}$$

$$dD = \left[\left(\frac{dD}{d\xi_D}\right) \frac{n_{ij} C_{ijkl}^e \left(n_{ij} n_{ij} - \frac{1}{3} n_{ii} n_{jj}\right)^{\frac{1}{2}}}{n_{ij} C_{ijkl}^e n_{kl} - \frac{\partial F}{\partial \xi}\left(\frac{\partial F}{\partial \sigma_{kl}} \frac{\partial F}{\partial \sigma_{kl}}\right)^{\frac{1}{2}}}\right]$$

$$d\varepsilon_{kl}^i = R_{ijkl} d\varepsilon_{kl}^i \tag{20}$$

or in the matrix notation,

$$\{d\sigma^a\} = [C^{DSC}]\{d\varepsilon\}' \qquad (21)$$

where J_{2D} is the second invariant of the deviatoric stress tensor, J_1 is the first invariant of the stress tensor, S_{ij} is the deviatoric part of the stress tensor σ_{ij}, δ_{ij} is Kronecker delta, and $[C^{DSC}]=[\Omega+\Psi+R^T(\sigma^C-\sigma^i)]$ is the DSC constitutive matrix.

3. Implementation of The DSC Model

The DSC model is implemented in a nonlinear finite element procedure based on the generalized Biot's theory for dynamics of saturated porous media. It includes a provision for simulating interfaces by using the thin-layer interface model. The finite element equation based on Eq. (17) is given by

$$\int_V([B]^T[C^{DSC}][B]dV)_n\{dq\}_n^i = \{Q\}_{n+1} - \int_V[B]^T\{\sigma\}_n^a dV \qquad (22)$$

where $[B]$ = transfortation matrix, $[C^{DSC}]$ = DSC constitutive matrix (see Eq. (21)), $\{q\}$ = vector of total displacements, $\{Q\}$ = load vector, $\{\sigma\}^a$ = observed shear vector, n = incremental stage. Thus Eq. (22) can be rewritten as

$$[K_n]\{dq\}_n^i = \{F_{n+1}\} \qquad (23)$$

where $[K_n]$ is the stiffness matrix at step n and $\{F_{n+1}\}$ is the unbalanced load. In the case of non-linear dynamic problems, $[K_n]$ and $\{F_{n+1}\}$ are defined using Newmark-β method and Newton-Raphson iterative scheme.

4. Laboratory Testing and Its Results

The test results (Alanazy and Desai, 1996) utilized in this study were obtained using a unique testing device, called the "Cyclic Multi-Degree-of-Freedom (CYMDOF-P) Testing Device." The CYMDOF-P shear device was designed to interface subjected to loads and displacements under a static nature or a time-dependant nature. The CYMDOF-P testing device is shown in Fig. 5. The details of the CYMDOF-P shear apparatus are shown in Fig. 6.

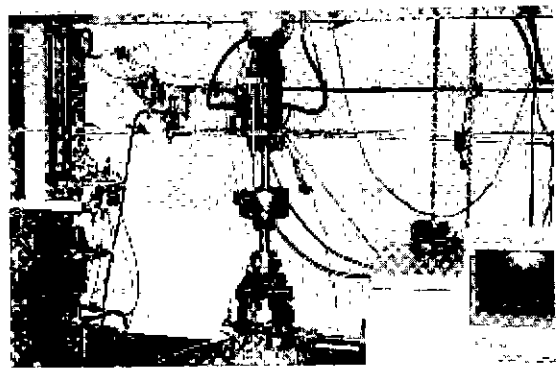

Fig. 5 CYMDOF-P testing device station (Alanazy, 1996)

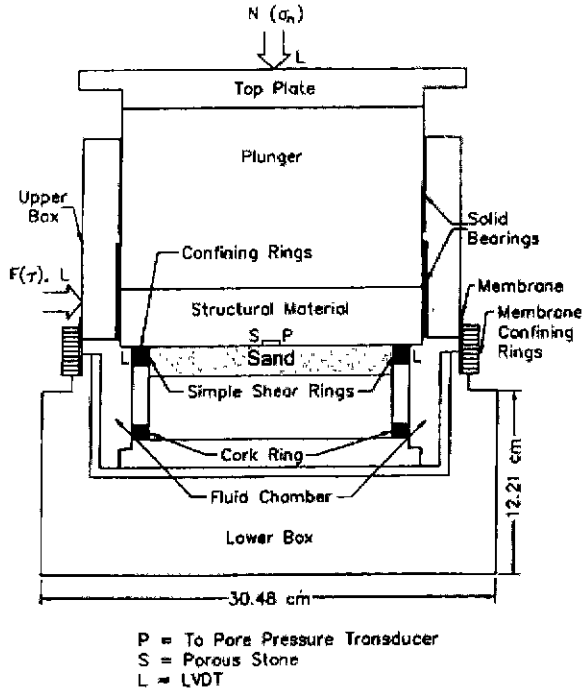

Fig. 6 A schematic representation of the CYMDOF-P apparatus

The interface system consists of the top sample, the interface, and the bottom sample. The top sample is the structural material (steel, in this paper) of a diameter of 20 cm and sits on the top of bottom sample (Ottawa sand, in this paper). Details of test procedures are given in User Manual (Rigby and Desai, 1995).

A total of six strain controlled simple shear tests data under one-way shear loading and two-way cyclic loading

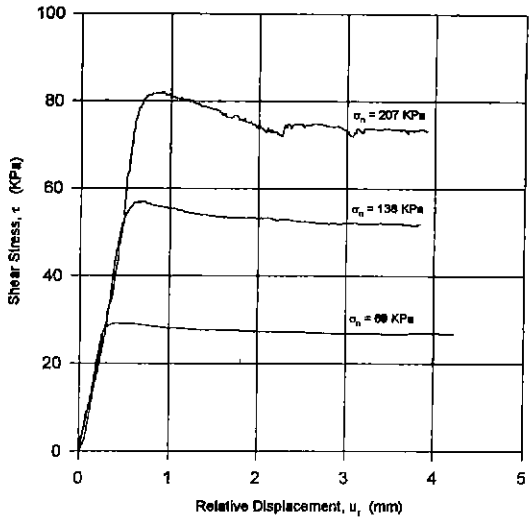

Fig. 7 Shear stress vs. relative displacement under one-way monotonic loading

conditions are used to evaluate the key parameters needed for the DSC model. Test data for saturated Ottawa sand and steel are shown in Fig. 7 and Fig. 8 (Alanazy and Desai, 1996).

Fig. 7 represents the relationship between the shear stress and the relative displacement under one-way monotonic loading with three different normal stresses (69kPa, 138kPa, and 207kPa) and a relative density (60%). It is clear that the maximum shear stress increases with the increase of the normal stress and occurred at a larger relative displacement. After reaching the peak stress softening was observed with the increase of the relative displacement. This behavior is also consistent with the critical concept of the medium dense sands. The softening behavior represented in three tests has an important role in soil-structure interaction and a typical example is the skin friction of a pile undergoing compression as a result of vertical loading.

Two-way cyclic loading is represent in the field under earthquake or wave loading. This type of loading is important, because it involves loading in the reverse direction that may involve severe changes in the behavior compared to any other type of loading. Under this type of loading, Ottawa sand and smooth steel interfaces were subjected to total displacement amplitude of 1.3mm.

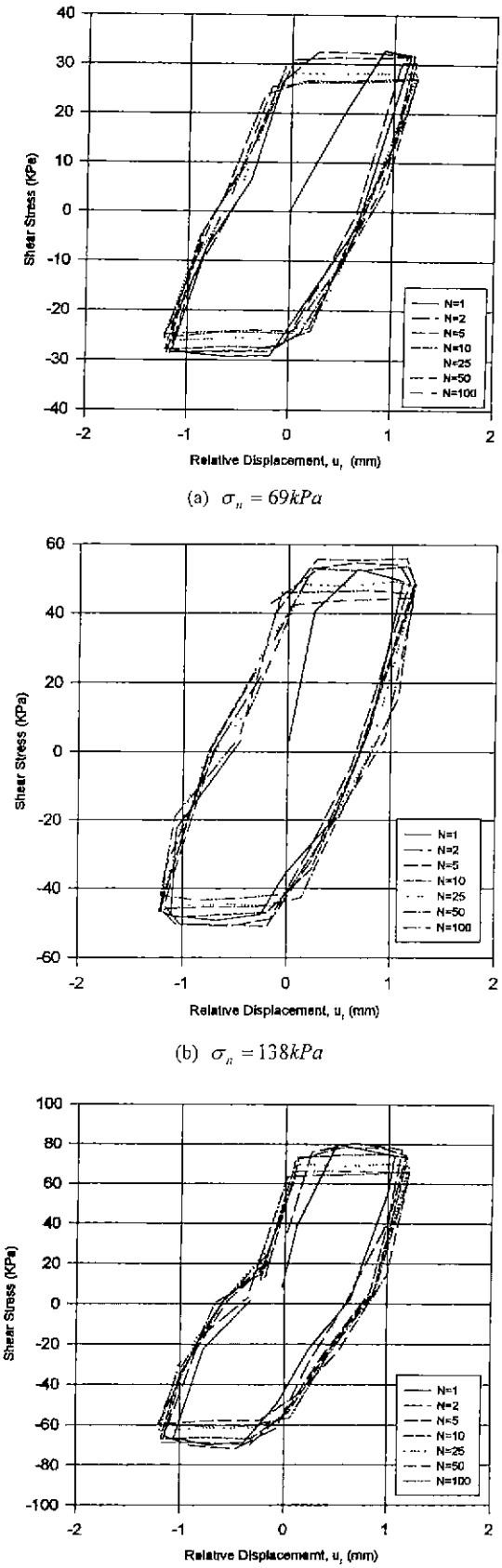

(a) $\sigma_n = 69kPa$

(b) $\sigma_n = 138kPa$

(c) $\sigma_n = 207kPa$

Fig. 8 Shear stress vs. relative displacement under two-way cyclic loading

Cyclic tests were performed with three different applied normal stresses (69kPa, 138kPa, and 207kPa) as shown in Fig 8. The rate of loading was 36.6mm/min in all of the tests. The results presented in this section are for cycle 1, 2, 5, 10, 25, 50, and 100.

The peak shear stress, in the positive direction, was observed in all of the three tests, which dropped to a mobilized shear stress when the total displacement amplitude was reached. There were no peak shear stresses observed under reverse loading and in the successive cycles. The mobilized shear stress in the negative direction was slightly smaller than the corresponding loading in the positive direction. The degradation of the mobilized shear stress is due possibly to the rotation of sand particular at the interface and change in the roughness of the steel surface with shear loading.

5. DSC Model Parameters

The parameters for the DSC model are determined from the foregoing cyclic CYMDOF-P shear tests. The parameters have physical meanings in that they are related to specific physical states during deformation; details of procedures for finding them are given elsewhere (Desai, 1995; park, 1997).

The parameters for steel-sand interface can be divided into four categories: Elasticity, RI (elasto-plasticity), FA (critical state), and Disturbance. The values of the DSC model parameters for the steel-saturated Ottawa sand interface are given Table 1. Brief descriptions for defining parameters are given below.

Table.1 Parameters for simulation of interface test (Park, 1997)

	Parameter	Saturated Sand Parameters	Interface Parameters
Elastic	E	193000 (kPa)	20531 (kPa)
Moduli	υ	0.380	0.384
Plasticity	n	2.450	3 400
Parameters	γ	0.123	0.274
Hardening	h_1	0 8450	0.8250
Parameters	h_2	0 0215	0.3180
Critical State	$\overline{m}$	0.150	0.35
Parameters	λ	0.020	0 0134
	e_n^c	0 601	0.580
DSC Function Parameters	A z	4.22 0.43	1.239 0 64

Intact State

Elastic parameters, E and [K_n], are found from the unloading slopes of τ vs. u_r and σ_n vs. v_r curves. These quantities are included in $[C^{ep}]$, the elasto-plastic matrix, Eq. (10). Ultimate parameter, γ, is found from $F=0$, Eq. (5), at the ultimate with $\alpha=0$:

$$\tau_{ult} = \sqrt{\overline{\gamma}}\,\sigma_n \qquad (24)$$

where τ_{ult} is ultimate asymptotic shear stress. The phase change parameter, n, is found based on the state of stress when transition from compact to dilative normal displacement occurs and $\partial F/\partial \sigma_n = 0$ shown in Fig. 3. And, the hardening or growth parameters, h_1 and h_2, are obtained by taking the natural logarithm of Eq. (6) as

$$\ln(\alpha) = \ln(h_1) - h_2 \ln(\xi_D) \qquad (25)$$

Knowing α and ξ_D, one can determine the best fitting line to the set of points ($\ln(\xi_D)$, $\ln(\alpha)$)to evaluate h_1 and h_2.

Critical State

The values of $\overline{m}$, Eq. (11), is the slope of σ_n^c vs. τ^c curve. Where τ^c is the shear stress at the critical state and σ_n^c is the corresponding effective normal stress. e_λ and λ are evaluated from the compression tests. e^c vs. $\ln\left(\frac{\sigma_n^c}{P_a}\right)$ is plotted and the best fitting is found. The value of intercept of the line is e_λ and the slope is λ.

Disturbance Function

Taking logarithm twice in Eq. (14) yields

$$\ln[-\ln(1-D)] = \ln(A) + Z\ln(\xi_D) \qquad (26)$$

At every stress point after the peak stress (τ, σ_n), ξ_D and D are known for several points. ln[-ln(1-D)]versus ln (ξ_D) curve can be plotted based on Eq. (26). The slope of

the average line represents Z and the intercept represents ln(A).

6. Boundary Value Problem

The two-dimensional two-phase (solid/fluid) dynamic finite element program (DSC-DYN_2D) with the proposed DSC model is verified by back predicting the interface test.

The interface tests (CYMDOF-P shear tests) under one-way monotonic and two-way cyclic loading are simulated by using the parameters found in the previous section. The sample is divided into 28 (4-node) elements (8 elements for steel plate, 4 elements for the interface, and 16 elements for sand) as shown in Fig. 9. The sample is fixed at the bottom. The displacement, both magnitude and rate as measured in the tests, are applied to both sides of sample. The parameters for saturated sand and interface are adopted from dynamic truly triaxial test data reported by Park (1997).

The test with σ_n = 138kPa under one-way monotonic loading was simulated where the constants used are obtained from Table 1. Fig. 10 shows the shear stress and relative displacement in the interface from the test result of CYMDOF-P shear test and the predicted result of finite element analysis. The correlation between the predicted response and the observed response is close, and there is reasonable since prediction is based on the parameters calculated from the actual test data.

The two-way cyclic loading tests with σ_n=138 kPa is

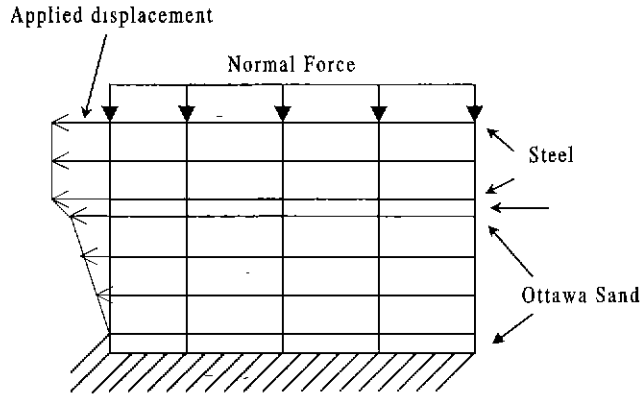

Fig. 9 Finite element mesh for interface

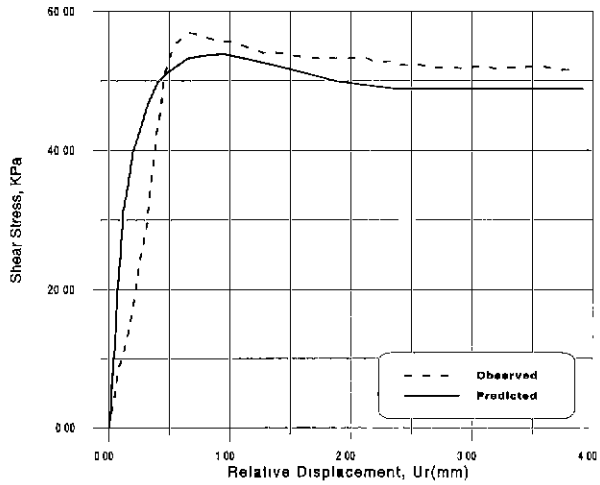

Fig. 10 The observed and predicted shear stress vs. relative displacement under one-way

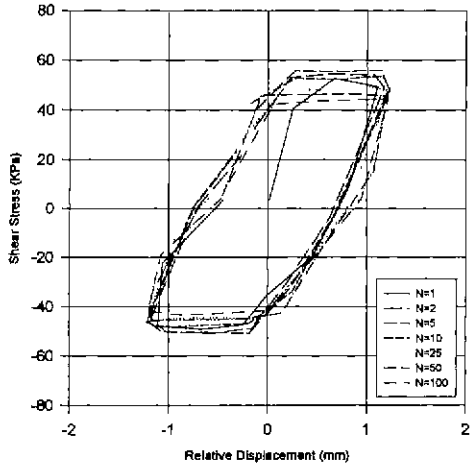

Fig. 11 The observed shear stress vs. relative displacement under two-way cyclic loading σ_n=207kPa

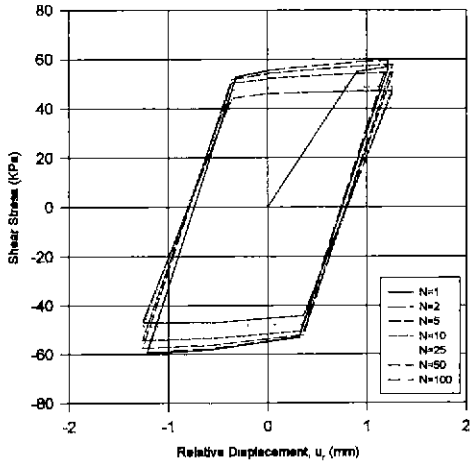

Fig. 12 The predicted shear stress vs. relative displacement under two-way cyclic loading (σ_n= 138kPa)

simulated by using parameters given Table 1. The actual behavior is shown in Fig. 11 while Fig. 12 presents the predicted behavior. The model backpredicts the observed behavior reasonably well. The degradation during cyclic is in good agreement with actual laboratory test data.

7. Conclusions

The Disturbed State Concept model, with HiSS model as the intact state and critical state as the fully adjusted state, were modified for interface and implemented in two phase dynamic finite element program, DSC-DYN2D. The applicability of this model has been demonstrated by back predicting laboratory tests for steel-saturated Ottawa sand interface.

It is shown that the finite element program, DSC-DYN2D, is capable for the saturated interfaces and dynamic analysis for geotechnical engineering problems. It can be used to solve the soil, soil-structure interaction, and structure problems in dry and saturated condition under static and dynamic loading.

References

1. Alanazy, A. S. (1996), "Testing and Modeling of Sand-Steel Interfaces Under Static and Cyclic Loading", Ph.D. Dissertation, Dept. of Civil Engrg. and Engrg Mech., Univ. of Arizona, Tucson, Arizona.
2. Armaleh, S. H. and Desai, C. S. (1990), "Modeling Include Testing of Cohesionless Soils Under Disturbed State Concept", Report to the NSF, Dept of Civil Engrg. and Engrg. Mech., Univ. of Arizona, Tucson, Arizona.
3. Desai, C. S. (1974), "A Consistent Finite Element Technique for Work-Sofening Behavior", Proc. Int. Conference on Computational Methods in Nonlinear Mechanics, Univ. of Texas at Austin, Austin, Texas.
4. Desai, C. S. (1980), "A General Basis for Yield, Failure, and Potential Functions in Plasticity", Int J Num. Analyt. Meth. in Geomech., Vol 4, pp. 361-375.
5. Desai, C. S. and Ma, Y. (1992), "Modeling of Joints and Interfaces Using the Disturbed State Concept", Int. J. Num. Analyt. Meth. in Geomech., Vol. 16, No. 9, pp. 623-653.
6. Desai, C. S., Park, I. J., and Shao, C. (1998), "Fundamental Yet Simplified Model for Liquefaction Instability", Int. J Num. Analyt. Meth. in Geomech., in press.
7. Desai, C S , Somasundaram, S., and Frantziskonis, G. (1986), "A Hierarchical Approach for Constitutive Modeling of Geologic Materials", Int. J. Num. Analyt. Meth. in Geomech., Vol 10, No. 3, pp 225-257.
8. Desai, C. S., Shao, C., and Park, I. J. (1997), "Disturbed State Modeling of Cyclic Behavior of Soils and Interfaces in Dynamic Soil-Structure Interaction", Proc., 9th IACMAG Conference, Wuhan, China
9. Desai, C. S., and Wathugala, G. W. (1987), "Hierarchical and Unified Models for Solids and Discontinuities (Joints/Interfaces)", Short Course Notes, Workshop on Implementation of Constitutive Laws of Engineering Materials, Dept. of Civil Engrg. and Engrg. Mech. Univ. of Arizona, Tucson, Arizona, pp. 9-10, 31-124
10. Park, I.J (1997), "Disturbed State Modeling for Dynamic and Liquefaction Analysis", Ph.D. Dissertation, Dept. of Civil Engrg. and Engrg. Mech., Univ of Arizona, Tucson, Arizona
11. Rigby, D. B. and Desai, C. S. (1995), "Testing, Modeling, and Application of Saturated Interfaces in Dynamic Soil-Structure Interaction", Report to the NSF, Dept. of Civil Engrg. and Engrg. Mech., Univ. of Arizona, Tucson, Arizona.
12. Roscoe, K. H., Schofield, A. and, Wroth, C. P. (1957), "On the Yielding of Soils", Geotechnique, Vol. 8, pp. 22-53.

(received on Apr , 19, 1999)